


Scaling eukaryotic cell-free protein synthesis achieved with the versatile and high-yielding tobacco BY-2 cell lysate

Mainak Das Gupta¹ | Yannick Flaskamp¹ | Robin Roentgen¹ | Hannes Juergens¹ | Jorge Armero-Gimenez^{1,2} | Frank Albrecht¹ | Johannes Hemmerich¹ | Zulfaquar Ahmad Arfi¹ | Jakob Neuser¹ | Holger Spiegel³ | Stefan Schillberg^{3,4} | Alexei Yeliseev⁵ | Lusheng Song⁶ | Ji Qiu⁶ | Charles Williams¹  | Ricarda Finnnern¹

¹LenioBio GmbH, Technology Centre, Aachen, Germany

²Laboratory of Nematology, Wageningen University and Research, Wageningen, The Netherlands

³Fraunhofer Institute for Molecular Biology and Applied Ecology IME, Aachen, Germany

⁴RWTH Aachen University, Institute for Molecular Biotechnology, Aachen, Germany

⁵National Institute on Alcoholism and Alcohol Abuse, National Institutes of Health, Rockville, Maryland, USA

⁶The Virginia G. Piper Center for Personalized Diagnostics, Biodesign Institute, Arizona State University, Tempe, Arizona, USA

Correspondence

Ricarda Finnnern, LenioBio GmbH, Technology Centre, Aachen 52074, Germany.
Email: r.finnern@leniobio.com

Funding information

Horizon 2020 Framework Programme, Grant/Award Number: 881025; Bundesministerium für Bildung und Forschung, Grant/Award Number: 0312B083OB

Abstract

Eukaryotic cell-free protein synthesis (CFPS) can accelerate expression and high-throughput analysis of complex proteins with functionally relevant post-translational modifications (PTMs). However, low yields and difficulties scaling such systems have prevented their widespread adoption in protein research and manufacturing.

Here, we provide detailed demonstrations for the capabilities of a CFPS system derived from *Nicotiana tabacum* BY-2 cell culture (BY-2 lysate; BYL). BYL is able to express diverse, functional proteins at high yields in 48 h, complete with native disulfide bonds and N-glycosylation. An optimized version of the technology is commercialized as ALICE[®] and advances in scaling of BYL production methodologies now allow scaling of eukaryotic CFPS reactions. We show linear, lossless scale-up of batch mode protein expression from 100 µL microtiter plates to 10 and 100 mL volumes in Erlenmeyer flasks, culminating in preliminary data from a litre-scale reaction in a rocking-type bioreactor. Together, scaling across a 20,000x range is achieved without impacting product yields.

Production of multimeric virus-like particles from the BYL cytosolic fraction were then shown, followed by functional expression of multiple classes of complex, difficult-to-express proteins using the native microsomes of the BYL CFPS. Specifically: a dimeric enzyme; a monoclonal antibody; the SARS-CoV-2 receptor-binding domain; a human growth factor; and a G protein-coupled receptor membrane protein. Functional binding and activity are demonstrated, together with in-depth PTM characterization of purified proteins through disulfide bond and N-glycan analysis.

Taken together, BYL is a promising end-to-end R&D to manufacturing platform with the potential to significantly reduce the time-to-market for high value proteins and biologics.

KEYWORDS

biomanufacturing, cell-free protein synthesis, eukaryotic post-translational modifications, N-glycosylation, protein biotechnology, scaling

1 | INTRODUCTION

Proteins are critical components of medicines, vaccines, and diagnostics. However, the design-build-test-learn cycles are too slow for protein research and manufacture using current cell-based methods. As highlighted by the recent COVID-19 pandemic, there is a need for end-to-end platforms that enable rapid research and development (R&D) pipelines with subsequently scalable manufacturing processes, to enable society to react rapidly to future threats to public health.

Cell-free protein synthesis (CFPS) has emerged as a powerful approach with the potential to enable accelerated R&D workflows, by first providing rapid and simple protein screening and later, the scaled production of promising protein leads (Carlson et al., 2012; Dondapati et al., 2020; Zawada et al., 2011). In comparison to cell-based expression, CFPS offers unprecedented speed with weeks of cell culturing, engineering, clone selection, and expansion, condensed into hours (Carlson et al., 2012; Swartz, 2012). Typically comprising a cell lysate or extract, a catalogue of CFPS platforms have been developed in the past decades and are defined by their starting cellular material. These include systems derived from bacterial, yeast, mammalian, and insect cell cultures, wheat germ extract (WGE), and reticulocytes from rabbit blood (Gregorio et al., 2019).

By decoupling the concerns of biomass accumulation and cell culture constraints from the essential mechanisms of recombinant protein production, CFPS offer unique advantages, such as the cytotoxic overexpression of membrane proteins and peptides which are often tightly regulated within intact cells (Schwarz et al., 2008; Xun et al., 2009; Xu et al., 2005). However, the widespread adoption of CFPS in therapeutic discovery pipelines has not materialized, due to: low product yields, inadequacies with installing post-translational modifications (PTMs) that are essential for correct folding and function of complex proteins, and a lack of scalability in cell lysate production methodologies and corresponding CFPS reactions.

A eukaryotic, coupled transcription-translation CFPS system based on tobacco BY-2 cell lysate (BYL) promises to overcome these issues. Following initial publications (Buntru et al., 2014, 2015), BYL has since been optimized and commercialized by LenioBio GmbH as ALiCE® (Almost Living Cell-free Extract). As BYL contains native, actively-translocating microsome vesicles derived from the endoplasmic reticulum and Golgi, it outperforms other CFPS modes in its capability of performing PTMs (Buntru et al., 2014, 2015). Simple addition of the melittin signal peptide (MSP) is sufficient for targeting to these microsomes. BYL reactions are also high-yielding in batch mode, bypassing complex and expensive continuous-exchange cell-free formats that are needed to make other eukaryotic CFPS reactions viable (Knauer et al., 2022; Stech et al., 2014; Thoring et al., 2017). Batch mode reporter protein yields of 3 mg/mL for the enhanced yellow fluorescent protein (eYFP) are notably higher than the maxima reported for previously established CFPS systems (Gregorio et al., 2019), specifically: 2.3 mg/mL green fluorescent protein (GFP) from *Escherichia coli* lysate (Caschera & Noireaux, 2014), 1.6 mg/mL GFP from WGE (Harbers, 2014), 0.25 mg/mL luciferase

from HeLa cell lysate (Mikami et al., 2006), and 0.05 mg/mL luciferase from a CHO cell lysate and two insect cell lysates (Brödel et al., 2014; Ezore et al., 2006). At the same time, the use of plant cell suspension cultures as the feedstock for lysate production combines with a relatively simple bioprocessing method to allow much better scaling potential compared to closely related eukaryotic CFPS systems for example, WGE harvested from full plant agriculture or expensive mammalian cell cultures in complex media formulations.

Indeed, recent advances in BYL manufacturing have allowed for scaling of the BYL CFPS reaction. Here, we show how this eukaryotic CFPS reaction can easily and linearly scale across a 1000x fold volume difference from 100 μ L reactions to 10 and 100 mL, for both the cytosolic reporter eYFP and the multi-domain microsomal glycoprotein glucose oxidase (GOx). Preliminary data from 1 L reactions from a commercial bioreactor are also disclosed, representing the first such example of litre scale reactions from a eukaryotic CFPS. No significant difference in yield was observed in direct comparison with 50 μ L reactions, highly remarkable considering the 20,000x fold volume difference and the batch mode reaction conditions.

Scaling of protein reactions consequently enables the purification of useful amounts of sample for more in-depth characterization of the proteins produced in BYL. Thus, we report the expression and characterization of an array of difficult-to-express proteins, specifically: GOx; a hepatitis B core virus-like particle (HBc-VLP), the monoclonal antibody adalimumab; the SARS-CoV-2 receptor-binding domain (RBD); human epidermal growth factor (hEGF), and a G protein-coupled receptor (GPCRs) membrane protein, cannabinoid receptor type 2 (CB2) (Figure 1). This panel features proteins of monomeric and multimeric nature, with disulfide bonds, N-glycosylation, and transmembrane domains, thus displaying the versatility of BYL. Importantly, we also present mass spectrometry analysis of disulfide bond formation and N-glycan structural characterization for some of these proteins. Such detailed analysis has never before been shown for proteins from eukaryotic CFPS, due to previous limitations in reaction volumes and yields. Here we found correct disulfide bond formation and high occupancy, homogeneous N-glycan profiles with high mannose structures typical of plant-derived recombinant proteins. Finally, these data are complemented by functional assays, to include surface plasmon resonance (SPR) binding analyses of adalimumab and hEGF against their cognate receptors, a serology-based ELISA of RBD against SARS-CoV-2 patient samples and a G protein activation assay using CB2 directly in the lysate matrix.

2 | MATERIALS AND METHODS

2.1 | Tobacco BY-2 cell culture and lysate production

Tobacco cells (*Nicotiana tabacum* L. cv. Bright Yellow-2; BY-2) were routinely cultivated in Murashige-Skoog liquid medium (MS)

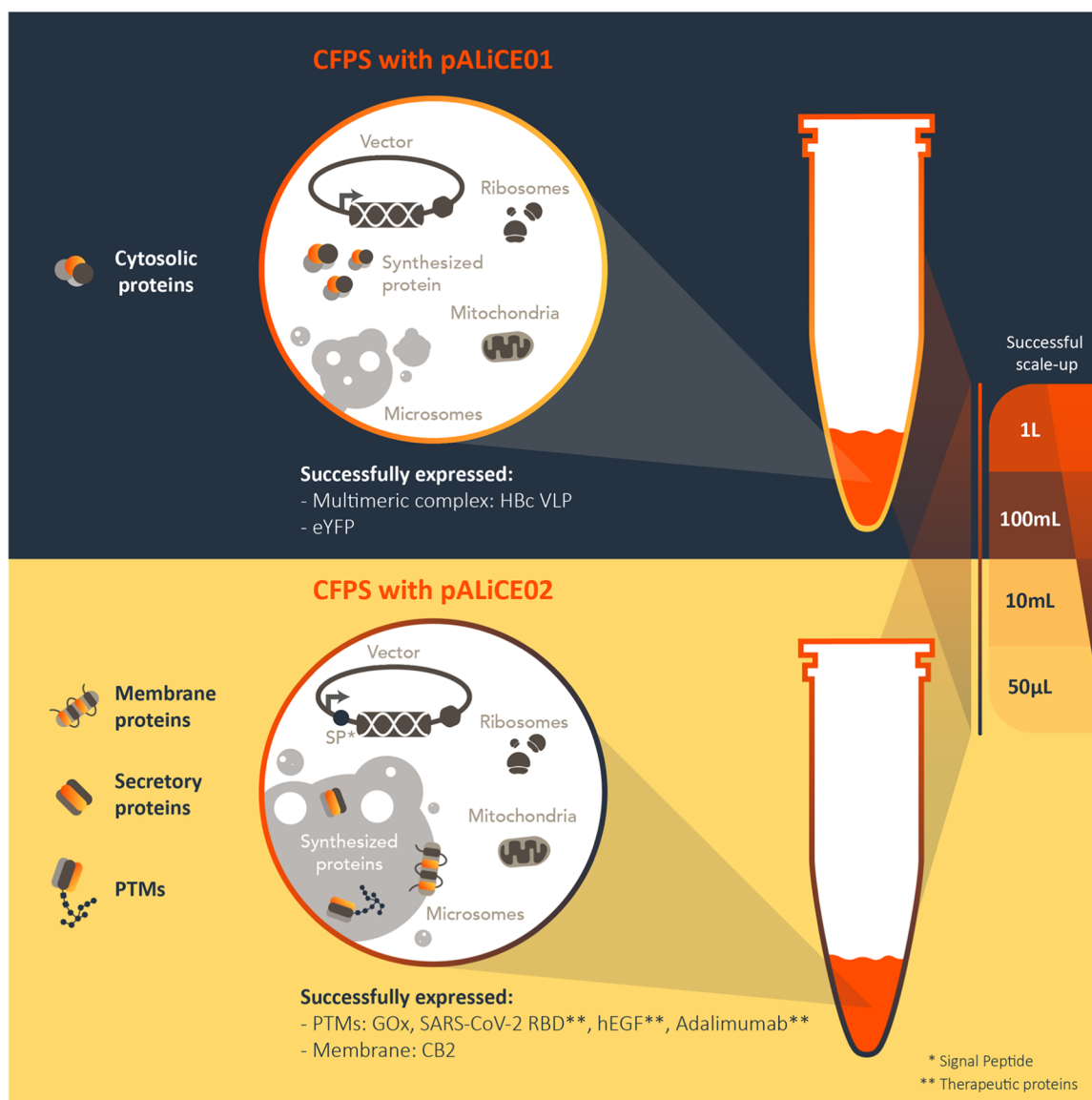


FIGURE 1 Cytosolic and microsomal protein expression in ALiCE. Cytosolic expressed proteins (top) include hepatitis B core antigen virus-like particle (HBc VLP) and enhanced yellow fluorescent protein (eYFP). Microsomal expressed proteins (bottom), include glucose oxidase (GOx), the receptor binding domain of the SARS-CoV-2 spike protein (RBD), human epidermal growth factors (hEGF), the antibody, Adalimumab, and the multi-pass transmembrane G protein-coupled receptor, cannabinoid receptor 2 (CB2).

at 1 L scale maintaining the exponential growth phase of the cells with a maximum packed cell volume of 40% at 26°C in the dark (Kirchhoff et al., 2012, 2020). Production cultures were inoculated 3.5% in MS medium supplemented with 2% (w/v) sucrose and Pluronic L-61 antifoam and cultured for 72 h at 26°C in darkness before lysate bioprocessing. Standard lysates were prepared from liter scale cultures. For the novel, scaled lysate bioprocessing methodology, larger culture volumes were obtained from cell culture seed trains generated in commercial bioreactors. General BY-2 lysate preparation has previously been described (Buntru et al., 2014, 2015). Scaled lysate production was performed using a novel, commercially sensitive method.

2.2 | Gene cloning and DNA template preparation

Genes encoding proteins of interest were purchased from gene synthesis providers (Integrated DNA Technologies, Inc.; Twist Bioscience) and transferred into pALiCE01 and pALiCE02 expression vectors (LenioBio GmbH; Supporting Information: Figures 2–3) using the Gibson DNA assembly method (Buntru et al., 2022). Vectors provided proteins of interest with N- or C-terminal Strep-II tags to enable facile downstream purification, except in the case of adalimumab where tag-less constructs were used. DNA fragments were amplified with 15–20 bp of homology regions in primers using Phusion R High Fidelity DNA polymerase (New England Biolabs; NEB) and homology based assemblies were performed using

NEBuilder® HiFi DNA Assembly Master Mix (NEB) following manufacturer's guidelines and transformed into *Escherichia coli* DH5- α cells. Correct clones were determined by sequencing and cultured for subsequent plasmid preparation using NucleoBond Xtra Midi/Maxi kits (Macherey-Nagel GmbH & Co. KG). For scaled CFPS reactions, milligram quantity production of template DNA was contracted to PlasmidFactory GmbH & Co. KG.

2.3 | CFPS reactions using BY-2 lysate

Generally, CFPS reactions were performed according to the ALiCE® instruction manual and published protocols (Buntru et al., 2022). Briefly, relevant volumes of BYL product were thawed in a room temperature water bath and template DNA added to final concentration of 5 nM (excepting the heteromeric adalimumab, whereby 5 nM of each heavy and light chain plasmids were used for a total DNA concentration of 10 nM). "Non-template controls" lacking DNA were always included to provide lysate background samples for downstream assays. Incubation temperature and runtime of 25°C and 48 h were used, irrespective of reaction volumes.

Microscale CFPS reactions of 50 and 100 μ L were performed in half-well and full well microtiter plates, respectively, using a humidified incubator with a platform shaking speed of 500 rpm and a shaking diameter of 12.5 mm. Additionally, Duetz system microtiter plate covers were used to limit uneven evaporation and edge effects (EnzyScreen BV). At the milliliter scale, reactions were optimized using Erlenmeyer type glass flasks. CFPS reactions of 10 and 100 mL were performed using sterilized 250 and 5000 mL flasks, respectively, with a shaking speed of 105 rpm. Finally, the 1 L scale reaction was performed using a CELL-tainer® CT20 rocking motion bioreactor with single-use bag. Agitation rate of 12 rpm and aeration at 300 mL/min yielded the best results here, with 20 rpm also trialed (Supporting Information: Figure 1).

2.4 | Reporter protein quantification

Expression of reporter proteins was quantified directly from lysate samples after CFPS reactions. For eYFP, lysate samples were diluted 1:10 with 20 mM MOPS buffer at pH 7.2 in microtiter plates. A calibration curve of eYFP standard was similarly prepared and the plate scanned for fluorescence signal with excitation and emission wavelengths of 485/20 and 528/20 nm, respectively, using an Infinite M1000 device (Tecan Group Ltd.). Quantification was achieved by subtracting raw fluorescence signals for non-template control from the values acquired for test samples and interpolating the adjusted value against the calibration curve.

GOx expression was quantified through a horseradish peroxidase (HRP)-coupled activity assay. Microsomal proteins were released by treatment of the lysate samples with 0.5% dodecylmaltoside (DDM) detergent for at least 15 min at room temperature. Samples were diluted 1:2500 in an assay buffer comprising 0.33 M glucose,

0.67 mM ABTS, and 1.67 U/mL HRP (Sigma-Aldrich) in 0.1 M potassium phosphate buffer at pH 6 in transparent 96-well plates. Absorbance over time at 420 nm was measured using the Infinite M1000 plate reader every 15 s over a period of 15 min. The linear absorbance increase over time was used to calculate sample GOx activity.

2.5 | SDS-PAGE and western blot analyses

Precast 4%–15% Mini-PROTEAN™ TGX Stain-Free™ (Bio-Rad Laboratories, Inc.) or NuPAGE 4%–12% Bis-Tris (Thermo Fisher Scientific) were used for SDS-PAGE. BYL volumes of 1 μ L were used to prepare samples. Stain-free gels were visualized under UV light but were otherwise stained with Coomassie brilliant blue R-250. PageRuler™ Plus Prestained Protein Ladder 10–250 kDa (Thermo Fisher Scientific) was used as molecular weight marker.

Proteins were transferred from gels to PVDF membranes using a Trans-Blot® Turbo™ Transfer System and associated accessories (Bio-Rad Laboratories, Inc.). Membranes were probed with anti-Strep-II tag and anti-CB2 antibodies according to manufacturer instructions.

2.6 | Production and transmission electron microscopy (EM) of VLPs

The human HBc (serotype adw) gene was cloned into the pALiCE01 vector, generating the pALiCE01-HBc plasmid. Microscale BYL reactions of 100 μ L reactions were performed using this template DNA. Resulting lysate samples were processed by centrifuging at 16,000 \times g for 10 min, to clarify the non-soluble fraction. Supernatant containing VLPs were collected and the non-soluble pellet resuspended in phosphate buffered saline (PBS). Each fraction was analyzed by SDS-PAGE.

For negative staining EM, formvar/carbon coated 400 mesh copper grids were exposed to a glow discharge in air for 20 s before applying 10 μ L of the VLP suspensions. Grids were incubated at room temperature for 2 min and negative staining was performed with 1% phosphotungstic acid, pH 7.2, for 1 min. The specimens were examined in a JEM-1400Flash Electron Microscope equipped with a Matataki Flash 2k x 2k camera (JEOL, Ltd.).

2.7 | CB2 expression and functional assay

The full-length human CB2 was expressed in *E. coli* as a fusion with the N-terminal maltose-binding protein (MBP), Strep-II tag and C-terminal deca-histidine affinity tags (MBP-StrepII-CB2-His₁₀), and human embryonic kidney (HEK) Expi239 cells without the MBP module (StrepII-CB2-His₁₀). Expression and purification from cell membranes was performed as previously described (Yeliseev et al., 2017, 2020). CB2 in complex with *E. coli* membranes was also

isolated. The MBP-StrepII-CB2-His₁₀ construct was cloned into pALICE01 and pALICE02 vectors for subsequent microscale expression in 50 μ L reactions. Resulting BYL samples and purified or membrane-bound CB2 proteins were analyzed by SDS-PAGE and western blot analysis with an anti-CB2 and anti-Strep-II antibodies.

Activation of G proteins by the recombinant CB2 was performed according to a previously reported protocol (Beckner et al., 2020). Briefly, BYL samples after CB2 expression or purified CB2 protein in Façade-TEG/CHS micelles were dispensed into pre-siliconized glass tubes containing 10 mM MOPS supplemented with 0.1% (w/v) BSA and 10 μ M CP-55,940 (Cayman Chemical). Upon addition of a mixture of G_{q11} (100 nM) and G_{12/13} (500 nM), the tubes were incubated on ice for 30 min. Reactions were completed to a total volume of 50 μ L with 50 mM MOPS buffer at pH 7.5, 1 mM EDTA, 3 mM MgCl₂, 4 μ M GDP, 0.3% w/v BSA, 100 mM NaCl, 1 mM DTT, and an appropriate amount of ³⁵S- γ -GTP, with tubes transferred rapidly to a 30°C water bath. Incubation continued for 20 min and reactions terminated by addition of 2 mL ice-cold stop solution TNMg (20 mM Tris-HCl pH 8.0, 100 mM NaCl, 25 mM MgCl₂). The reaction was rapidly filtered through 0.45 μ m nitrocellulose filters. Filters were washed with 4 \times 2 mL of cold TNMg buffer, dried, placed into scintillation vials and counted upon addition of ScintiSafe Econo F scintillation liquid (Fisher).

2.8 | Purification of microsomal proteins from BYL lysate

Medium scale reactions of 10 mL were used to express hEGF, adalimumab, GOx, and SARS-CoV-2 RBD from pALICE02 vectors. Following the CFPS reaction, lysates were centrifuged at 16,000 \times g for 20 min at 4°C to pellet the microsomal fraction. Microsome pellets were resuspended in 0.5% DDM in PBS to the original volume of the reaction and incubated for at least 15 min at room temperature to disrupt the microsome and release the soluble protein. Suspensions were then clarified by a repeated centrifugation step and the supernatant progressed for purification.

nProtein A Sepharose 4 Fast Flow resin (Cytiva) was used for affinity purification of adalimumab whilst Strep-Tactin XT 4Flow resin (IBA Lifesciences) was used for Strep-II tagged-tagged proteins. Purifications were performed manually according to manufacturer instructions and resulting elutions were concentrated and buffer exchanged to PBS using Amicon Ultra Centrifugal Filter Units (Merck). Purified, concentrated protein samples were calculated by comparing absorbance measurements against theoretical molar extinction coefficients for specific proteins.

2.9 | Analytical size exclusion chromatography

Size exclusion-high-performance liquid chromatography (SEC-HPLC) analyses of protein purity were obtained with a 1260 Infinity II Bio-Inert system (Agilent). Adalimumab and GOx samples of 1 mg/mL

were injected to a Superdex 200 Increase 5/150 GL column (Cytiva; 3.0 mL void volume) equilibrated with 50 mM sodium phosphate, 150 mM NaCl pH 7.2. A flow rate of 0.45 mL/min and runtime of 10 min were used to separate samples with UV-Vis absorbance readings at 280 nm.

2.10 | SPR analyses

SPR spectroscopy was conducted on a Biacore T200 instrument (Cytiva). HBS-EP+ at pH 7.4 (Biacore/Cytiva) was used as the running buffer, with measurements were conducted at 25°C and at a flow rate of 30 μ L/min. For capture of antibodies and Fc-Fusions a CM5-S-Series sensor chip (Cytiva) was functionalized with 2500RU recombinant Protein A (Sigma) using EDC/NHS Coupling Kit (Biacore/Cytiva BR-1000-50) according to the manufacturer's suggestion. Flow cell one (Fc 1) was activated and deactivated to be used as a reference for blank subtraction. Between the measurement cycles, the surface was regenerated by pulsing for 45 s with the recommended regeneration buffer (10 mM glycine-HCl pH 2.1 supplied within the Human Fab Capture Kit). Buffer injections were used for double referencing.

Kinetic parameters were determined for the interaction of BYL-derived adalimumab batches as well as commercial Humira® (antibodies-online) with the corresponding antigen tumor necrosis factor (TNF- α ; Abcam plc), as well as with the human FcR I (CD64; R&D Systems) receptor. Antibodies were captured by injecting an appropriate dilution of each respective molecule in running buffer for 180 s, followed by an injection of either TNF- α or CD64 for 180 s followed by a 420 s dissociation phase and a 45 s regeneration step using 30 mM HCl. The cycle was repeated with eight serial twofold dilutions of the respective ligands, starting at 60 nM for TNF- α and 30 nM for hCD64. Affinity constants were determined through fitting the resulting sensograms with the BiacoreEval 3.0 software after performing double-referencing using the Biacore T200 evaluation software. A 1:1 binding model was used.

A similar approach was used to quantify the interaction between BYL-derived hEGF and a standard from *E. coli* (R&D Systems) with recombinant epidermal growth factor receptor (EGFR) Fc-fusion (R&D Systems). EGFR was captured by injecting an appropriate dilution of the molecule in running buffer for followed by injection of the hEGF samples following the parameters outlined above. The cycle was repeated with five serial twofold dilutions of the ligands, starting at 41.6 nM. Affinity constants were determined as above.

2.11 | Deglycosylation assay, SDS-PAGE, and immunoblot

Deglycosylation with either EndoH or PNGaseF (NEB) was performed according to the manufacturer's instructions. Aliquots of purified proteins were treated with either EndoH or PNGaseF, followed by SDS-PAGE analysis.

2.12 | N-glycan and disulfide bond analyses via mass spectrometry

For N-glycopeptide analyses, purified protein samples were prepared by S-alkylation with iodoacetamide and digestion with either with LysC/GluC (Promega) [RBD] or, in the case of adalimumab, trypsin (Promega). Samples were loaded on a nanoEase C18 column (nanoEase M/Z HSS T3 Column, 100 Å, 1.8 µm, 300 µm × 150 mm, Waters) using 0.1% formic acid as the aqueous solvent. A gradient from 1% B (B: 80% Acetonitrile, 0.1% FA) to 40% B in 50 min was applied, followed by a 10 min gradient from 40% B to 95% B that facilitates elution of large peptides, at a flow rate of 6 µL/min. Detection was performed with an Orbitap MS (Exploris 480; Thermo Fisher Scientific) equipped with the standard H-ESI source in positive ion, DDA mode (=switching to MSMS mode for eluting peaks). MS-scans were recorded (range: 350–1200 Da) and the 20 highest peaks were selected for fragmentation. Instrument calibration was performed using Pierce FlexMix Calibration Solution (Thermo Fisher Scientific). The possible glycopeptides were identified as sets of peaks consisting of the peptide moiety and the attached N-glycan varying in the number of HexNAc units, hexose, deoxyhexose, and pentose residues. The theoretical masses of these glycopeptides were determined with a spread sheet using the monoisotopic masses for amino acids and monosaccharides. Manual glycopeptide searches were made using Freestyle 1.8 (Thermo Fisher Scientific). For the quantification of the different glycoforms the peak areas of Extracted Ion Chromatograms of the first four isotopic peaks were summed, using the quantification software Skyline.

Disulfide bond analysis workflows were conducted similarly. Protein samples were S-alkylated and processed with pepsin or, in the case of adalimumab, AccuMAP™ Low pH

Protein Digestion Kit (Promega) according to the manufacture's protocol. The digested samples were loaded on a nanoEase C18 column with separation and detection and separated using identical parameters as above. The files were searched against databases containing the primary sequences for the full-length proteins.

2.13 | SARS-CoV-2 RBD binding and serological assay

Anti-RBD antibodies were procured to recognize either linear or conformational epitopes (MAB10540 and MAB105802, respectively; R&D Systems). Serum samples were collected either from COVID-19 patients with a positive PCR test in 2020 or before 2019 as negative controls. HaloTag-GST was used as a negative control antigen (Promega).

Pure protein samples were coated to microtiter plates overnight with 4°C incubation at a concentration of 2 µg/mL. After washing with 0.2% Tween-20 in PBS (PBST) and blocking with PBST-1% BSA, antibodies at 1:10,000 dilution or serum samples at 1:200 dilution were introduced and incubated at room temperature for 1 h. After further 0.2% PBST washing, HRP-conjugated anti-mouse IgG or anti-human IgG detection antibodies (Sigma) were added at 1:10,000 dilution with a final room temperature incubation for 1 h. Plates were then developed with

3,3',5,5'-tetramethylbenzidine substrate and absorbance readings at 450 nm measured using an Envision plate reader.

3 | RESULTS

3.1 | Linear scalability of CFPS reactions in BYL

BY-2 cell lysate (BYL) is commercialized as the product ALiCE®, optimized for the capability to produce 3 mg/mL of the cytosolic reporter protein eYFP in batch mode sub-milliliter volume reactions from the pALiCE01 plasmid (Figure 2a). This yield in small volumes is ideal for screening and research purposes and the system is pre-supplemented with T7 RNA polymerase and the reaction mixture, in contrast to other systems that require a supplementation step at the point of use. However, significantly larger reaction volumes are necessary to produce proteins at the amounts required for industrial applications. Scaling of CFPS systems first requires scaling of the cellular input material fermentation volumes and of the lysate production process, to generate sufficient lysate material to allow for scaling of the actual CFPS reaction. This reaction scaling requires an exploration of reaction vessels, oxygen transfer rates (OTR), and other protein expression reaction conditions (Gregorio et al., 2019).

Scaled BY-2 culture and lysate production has been achieved and now permits liter scale BYL production. Thus, we were able to test the consistency of BYL performance across reaction volumes of 0.1, 10, and 100 mL using just two large batches of lysate for all scaling experiments. Cytosolic pALiCE01 and microsomal pALiCE02 vectors encoding the reporter proteins eYFP and GOx, respectively, were used as template DNA material for 48 h cytosolic and microsomal CFPS reactions at these different scales (Figure 2b). eYFP and GOx titers demonstrated strikingly linear scalability from 0.1 to 100 mL reaction volumes, demonstrating a scaling factor of 1000x with no significant loss of protein yield at the reaction endpoint, regardless of expression mode and protein. Maximum eYFP yields of 1.5 mg/mL were reached from these research-grade lysate batches, somewhat less than the commercial-grade ALiCE® product. Owing to the lack of a well-characterized GOx standard, microsomal yields are presented as a function of activity and enzyme units. Here, maximum yields are ~55 U/mL, a 7.5x increase from the yields initially determined for unoptimized BYL (Buntru et al., 2015). Together, these data represent the largest eukaryotic CFPS reactions to date and the linear scaling supports the use of BYL as an end-to-end R&D platform, whereby protein engineering can be performed at the microliter scale before undemanding upscaling.

For 0.1 mL expressions, microtiter plates were used, whilst orbitally shaken Erlenmeyer-type glass flasks were chosen as milliliter scale reaction vessels due to the universality of this glassware and the availability of characterization data regarding the OTR (Bü et al., 2000; Maier & Büchs, 2001). An optimal OTR_{max} of above 18 mmol/L/h was determined for BYL in microtiter plate reactions (data not shown). Erlenmeyer flask sizes of 250 and 5000 mL were thus chosen as they could achieve this OTR_{max} at the same shaking

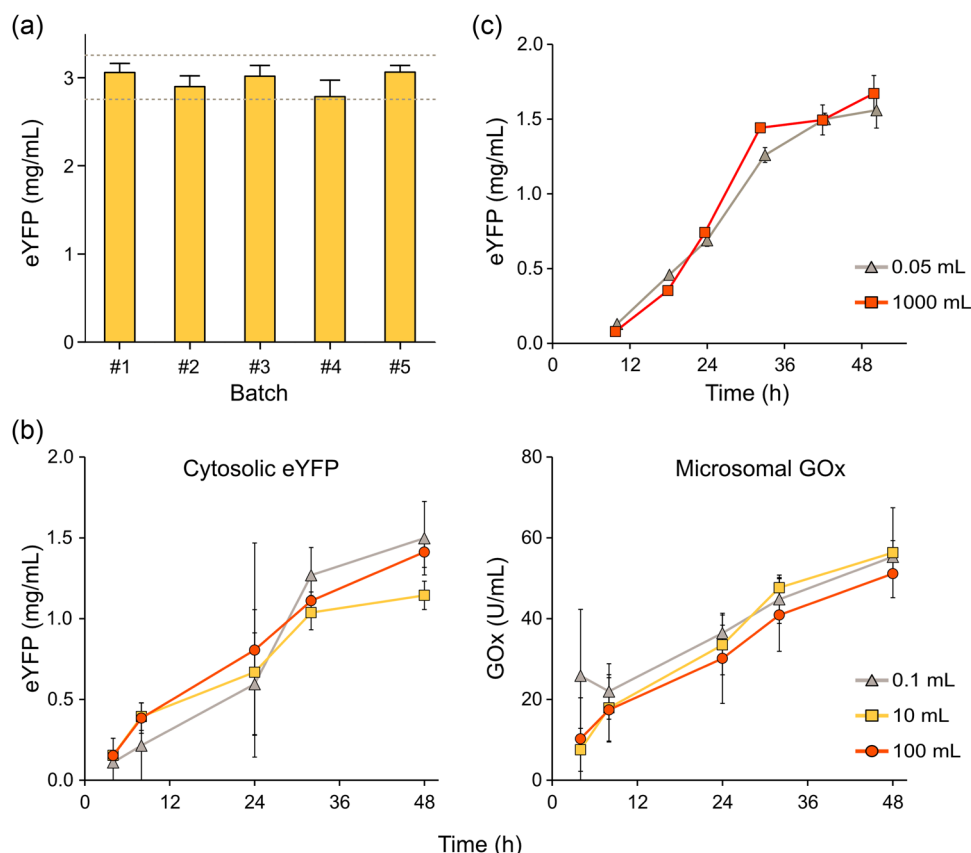


FIGURE 2 Scaling cell-free protein synthesis reactions using BY-2 lysate. (a) eYFP expression yields in recent commercial batches of ALiCE[®] from 50 μ L half-well microtiter plate reactions. Fluorescence of lysate samples are compared against eYFP standards to calculate yields and batch release quality control criteria of 2.7–3.3 mg/mL are indicated. (b) Cytosolic and microsomal protein expression scaling at 0.1, 10, and 100 mL using research-grade BY-2 cell lysate. CFPS reactions were performed in either microtiter plates or shake flasks for 48 h and at 25°C, with eYFP and GOx concentrations determined by fluorescence and colorimetric activity assays, respectively ($N = 2$). (c) Preliminary trial of a 1000 mL CFPS reaction for cytosolic eYFP production. Comparison with microtiter plate reactions of 50 μ L show no significant difference between protein yield across a scaling factor of 20,000x. CFPS, cell-free protein synthesis; eYFP, enhanced yellow fluorescent protein; GOx, glycoprotein glucose oxidase.

frequency of 105 rpm (Supporting Information: Table 1). Mixing times were not empirically determined here but previous reports suggest these to be negligible (<10 s) for shake flasks at these milliliter scale volumes (Tan et al., 2011).

Considering no difference in scalability potential between the simple, cytosolic eYFP and the complex, microsomal GOx, it is not expected that these conditions need further optimization when moving across the micro-milliliter scale. However, to truly achieve manufacturing potential for high value proteins, eukaryotic CFPS reactions must also be scaled to liters and potentially kiloliters in the future. Thus, we also present the results of preliminary trials comparing 50 μ L microplate reactions to a 1 L BYL reaction using the CELL-tainer[®] CT20 commercial bioreactor (Figure 2c). Remarkably, timecourse data reveals that eYFP yields were practically identical throughout the 48 h runtime, regardless of reaction scale. Vendor-supplied data states that 12–16 s can be expected at a 12 L working volume for this device (Oosterhuis & Junne, 2013–2014). Some initial optimization of agitation speeds was also performed using 0.3 L volumes of BYL, with 12 rpm chosen as the more gentle

setting that was equally able to achieve maximum eYFP yield of the lysate in the 48 h reaction (Supporting Information: Figure 1). The consistency of CFPS yields across this scaling factor of 20,000x is a clear indication of the potential for this eukaryotic CFPS system and a deeper investigation of BYL reaction scaling is ongoing, where scaling parameters and mixing times will be validated with a broad range of commercially available, widespread bioreactors that use stirred-tank or wave motion working principles. The idea is to preempt the usual process development that first-time BYL users might face to further lower the barrier to entry for this simple system.

3.2 | Expression of multisubunit protein complexes in BYL with in-depth molecular and functional characterization

VLPs are complex nanostructures built by the specific interaction between hundreds of virus-derived protein monomers. As they closely resemble viruses but are unable to infect the host cell due to

absence of viral genetic material, VLPs can be utilized in medicine as potent and safe vaccines (Tariq et al., 2022). Furthermore, VLPs may serve as delivery vectors for RNA/DNA vaccines or targeted drug delivery (Nooraei et al., 2021). Production of VLPs by CFPS has the added advantage that reaction parameters can be readily modified to improve VLP assembly rates. However, previously published efforts with eukaryotic CFPS have struggled to achieve useful yields in meaningful reaction volumes. In the case of the Hepatitis B core antigen model VLP (HBc), *Pichia pastoris* and WGE systems have yielded only 6.4 and 4 µg/mL VLP production, respectively, and neither system was used beyond the microliter scale for HBc (Aw et al., 2020; Lingappa et al., 1994; Spice et al., 2020).

Using the BYL CFPS system, high concentrations of fully assembled HBc VLP were obtained after a 48 h reaction, without the need for further optimization. SDS-PAGE analysis first confirmed the presence of the 21 kDa monomer in the lysate and after purification (Figure 3a). In-gel quantification gave an estimated HBc monomer yield of 1 mg/mL, representing 150-fold increases over other eukaryotic CFPS reports. Electron micrographs confirmed the presence of a homogeneous population of fully-formed VLPs in the lysate (Figure 3b). The BYL also outperformed HBc yields of 0.4 mg/mL from an *E. coli* CFPS system (Colant et al., 2021). These results show the potential of BYL to produce high-yields of multimeric complexes like VLPs. Since initial submission of this article, a more developed story for HBc VLP expression in BYL has been published, to include further lossless scaling comparisons across 0.05–1000 mL reaction volumes with subsequent VLP purification and immunogenicity assays by quantification of released cytokines from human peripheral blood mononuclear cells (Armero-Gimenez et al., 2023).

Additional multisubunit model proteins were selected for further study of folding and PTMs capabilities, namely: the enzyme GOx, a homodimer comprised of 80 kDa monomers that are covalently linked by disulfide bonds and each possessed of 8 N-glycosylation sites; and the therapeutic monoclonal antibody adalimumab (Humira®), a complex heterotetramer of 150 kDa comprised of two heavy and two light chains, together containing two N-glycosylation sites, 12 intramolecular and four intermolecular disulfide bonds. Adalimumab heavy and light chain genes were cloned directly into pALICE02 vectors for microsomal targeting whilst RBD and GOx genes were prepared similarly with additional N-terminal Strep-II tags for purification. Proteins were expressed in 10 mL reactions using triplicate, independent batches of BYL and the resulting microsomes were processed by DDM detergent treatment for protein release and subsequent Protein A or streptavidin affinity purification.

For adalimumab, a 1:1 ratio of heavy and light chain pALICE02 plasmids was sufficient to produce full-length IgG molecules at the expected 150 kDa mass (Figure 3c). Analytical size-exclusion chromatography resolved a single major peak for Adalimumab expressed in ALICE indicating a homogeneous population of heterotetrameric mAb (Figure 3d). Indeed, a near-perfect overlay was observed between the chromatograms of Adalimumab produced cell-free in ALICE as well as in CHO cells. Intermediate assemblies of heavy and light chain visible in the nonreducing PAGE (Figure 3c) were probably

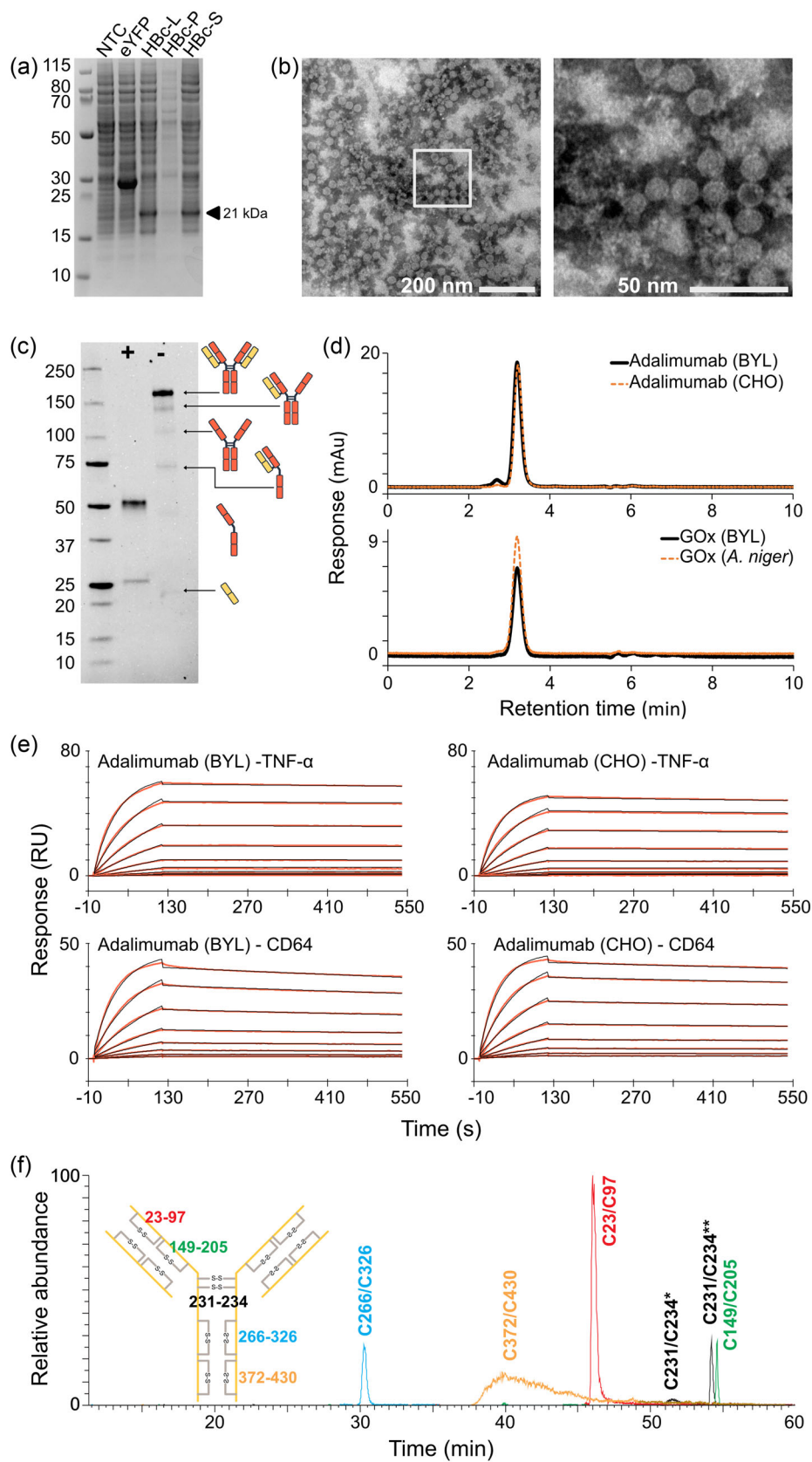
caused by partial disulfide bond disruption during protein migration through the gel matrix. Similarly comparable SEC profiles with single major peaks were seen for GOx expressed in BYL and a commercial standard purified from *Aspergillus niger*, indicating homogeneous dimeric protein molecule with no misprocessed variants or monomeric species observed for either sample (Figure 3d).

The functional binding activity of adalimumab samples toward the TNF-α ligand and the Fc-gamma receptor CD64 was assessed by SPR in a comparison with a commercial adalimumab reference product from CHO cells (Figure 3e). For TNF-α binding, BYL-mAb demonstrated slightly stronger affinity than CHO-mAb, with an average K_D (M) value of 1.34×10^{-10} compared to 1.85×10^{-10} , respectively. Conversely, BYL-mAb showed weaker binding to the CD64 receptor than CHO-mAb (3.53×10^{-10} compared to 1.58×10^{-10}). Considering that the adalimumab mechanism of action is the neutralization of free TNF-α, this enhanced ligand binding and weaker receptor binding may combine for an improved therapeutic effect when this monoclonal antibody is produced in BYL compared to mammalian cell systems. Disulfide bond analysis of adalimumab was also used to demonstrate the correct formation of the expected intra- and intermolecular bonds (Figure 3f).

3.3 | N-linked glycosylation of glycoproteins expressed in BYL

To assess the N-glycosylation potential of the eukaryotic BYL a panel of glycoproteins was used, to include adalimumab and GOx, together with the RBD of the SARS-CoV-2 spike, a monomer of 25 kDa with four intramolecular disulfide bonds and two N-glycosylation sites (Figure 4). RBD was also produced with the HaloTag in different C-terminal positions and the full-length spike protein S1 was also expressed. Similar to previous reports of glycoproteins produced by eukaryotic CFPS (Thoring & Kubick, 2018), the presence of N-glycosylation is first demonstrated using simple SDS-PAGE mobility shifts after glycosidase treatment with either Peptide:N-glycosidase F or Endoglycosidase H (PNGase F and EndoH, respectively; Figure 4b). Gel migration differences were equal for both glycosidases, suggesting high mannose and hybrid N-glycans are predominant. However, there has been no detailed analysis on the composition of N-glycans from proteins produced via eukaryotics CFPS as the requisite sample amounts for mass spectrometric characterization were unobtainable. Successful scaling of the BYL system has enabled sufficient sample amounts for more in-depth examination and so we analyzed the N-glycan structures of the GOx, RBD, and adalimumab preparations that were also used for disulfide bond characterization.

N-glycopeptide digestions were followed by liquid chromatography electrospray ionization tandem mass spectrometric identification and assignment of structures (LC-ESI-MS/MS; Figure 4d). The analysis revealed a high degree of N-glycosylation occupancy and reproducibility across batches, regardless of the protein model. The N-glycan profile is broadly consistent across all N-glycosites and demonstrates a dominant mannose 8 (Man8) species. Similarly to

**FIGURE 3** (See caption on next page)

recombinant proteins produced in whole *Nicotiana* spp. plants, plant-specific glycosylation features of α 1,3-fucosylation and β 1,2-xylosylation were also observed at some N-glycosites, especially within the RBD protein. One glycosylation position on the GOx protein was not detected and, therefore, not characterized. This site was located within a weakly charged peptide of approximately 50 amino acids, presumed to have hindered detection within the mass range of the MS instrument.

3.4 | Functional expression of a multi-pass transmembrane GPCRs, CB2

Integral membrane proteins are challenging for recombinant expression due to a number of specific requirements for folding, PTMs, and insertion of these proteins into cell membranes or detergent micelles (Bernaudat et al., 2011; Grisshammer, 2006). GPCRs are one of the largest classes of integral membrane proteins involved in a wide array of signal transduction and regulatory pathways in the human body, and therefore attract significant attention. However, despite significant efforts over the past two decades, there has been limited success in expressing correctly folded and functionally active GPCR in CFPS systems (Orbán et al., 2015). An improved methodology has been described for functional *E. coli* expression of the class A rhodopsin-like GPCR human CB2, as well as from mammalian HEK293 and CHO cell cultures (Beckner et al., 2020; Yeliseev, 2019; Yeliseev et al., 2020). However, no successful CFPS of the CB2 receptor has been reported.

Figure 5 presents proof of functional CB2 expression in BYL. The 44 kDa CB2 was expressed from both pALiCE01 and pALiCE02 vectors as a fusion with the N-terminal MBP of *E. coli*, a Strep-II tag and a C-terminal His-tag—the same construct that was successfully developed for bacterial and mammalian cell-based expression (Yeliseev et al., 2017). BYL expression reactions of 50 μ L were performed and MBP-CB2 expression levels then measured by western blot, with function demonstrated by quantitative activity assays. The western blot image (Figure 5a) shows BYL reaction products, probed with anti-CB2 (left panel) and anti-Strep-II tag (right panel) antibodies, and confirms that MBP-CB2 is well expressed from both pALiCE01 and pALiCE02 vectors.

Functional activity of the expressed MBP-CB2 protein was assessed in the lysate by measurement of G protein activation rates

upon binding of the receptor with the synthetic cannabinoid agonist CP-55,940 (Figure 5b). Remarkably, functional protein was found from both pALiCE01 and pALiCE02 expression vectors, possibly suggesting a passive loading mechanism of the protein to microsomal membranes in the former case, independent of the MSP-led microsomal translocation pathway. Comparison with recombinant MBP-CB2 purified from *E. coli* gives approximate BYL yields of 150–200 μ g/mL without any optimization of reaction conditions or the addition of supplementary lipids, detergents, or nanodiscs that are required for other CFPS systems without native membrane compartments. The MBP solubility tag was used here to generate directly comparable data with MBP-CB2 purified from cell-based sources. However, BYL expression of membrane proteins without solubility tags is also straightforward (data not shown).

3.5 | Functional expression of therapeutic proteins—a SARS-CoV-2 vaccine subunit candidate and hEGF

CFPS is well suited to the study of emerging pathogens, with rapid expression times that can outpace even quickly mutating threats. A concerted, global research effort was essential for mitigating the recent SARS-CoV-2 pandemic but a preponderance of expensive, low quality commercial antigen samples did not help. Antigens from mammalian cells, yeast cells and baculovirus-insect cells proved costly and too low yielding to support vaccine or therapeutic development, while antigens derived from heterologous *E. coli* expression were highly available but lack the PTMs of the disease-relevant proteins (He et al., 2021). Herein we have shown the BYL system to be capable of producing recombinant SARS-CoV-2 spike protein RBD within 48 h and with consistent batch-to-batch N-glycosylation. The RBD was expressed in BYL and purified from BYL with a high degree of purity (Figure 6a). The sample that was used for N-glycopeptide analysis was also subject to disulfide bond analysis, again confirming that BYL produces proteins with the correct folding (Figure 6b).

This protein is considered an important target for developing a SARS subunit vaccine. Indeed, the majority of the potent neutralizing antibodies against SARS-CoV-2 target the RBD (Piccoli et al., 2020), but reports differ on whether RBD alone or full S1 subunits of the spike are more potent vaccines in terms of IgG and IgA induction (Dickey et al., 2022; Min & Sun, 2021). To explore this concept, we expressed both RBD and this S1 subunit from the pALiCE02 vector

FIGURE 3 Production, characterization, and functional assessment of multisubunit complexes in BY-2 lysate (BYL). (a) SDS-PAGE of BYL samples after expression of the hepatitis B core antigen (HBc) protein. The expected 21 kDa band of the monomer is indicated by the arrow. (b) Electron microscopy picture of negatively stained, self-assembling virus-like particles in BYL. (c) Native PAGE of purified adalimumab electrophoresed under reducing (+) and nonreducing (–) conditions. (d) SEC-HPLC analysis of adalimumab and GOx produced in BYL compared to commercial standards. (e) SPR analysis of adalimumab and its binding partners. Immobilized antibody molecules produced from either BYL or CHO cells were probed with recombinant TNF α and CD64 to show ligand and receptor binding, respectively. (f) Disulfide bond analysis of adalimumab. eYFP, enhanced yellow fluorescent protein control reaction; GOx, glycoprotein glucose oxidase; HBc-L, total lysate after expression; HBc-P, insoluble fraction pellet; HBc-S, soluble protein fraction; NTC, non-template control; SEC-HPLC, size exclusion-high-performance liquid chromatography; SPR, surface plasmon resonance.

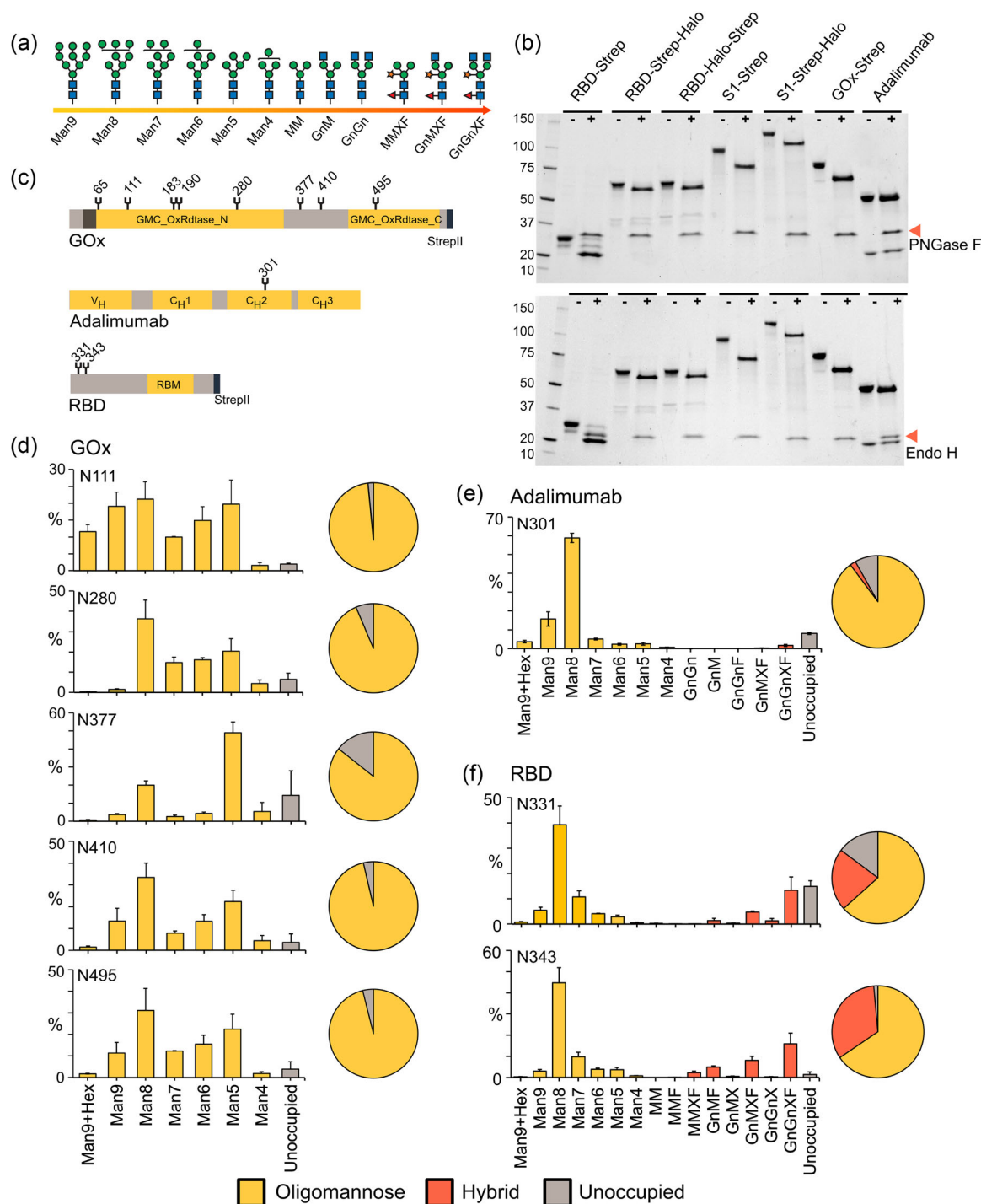


FIGURE 4 N-glycosylation investigation of proteins produced in BYL. (a) Schematic explanation of N-glycan structures and nomenclature. (b) SDS-PAGE mobility shift after glycosidase treatment. (c) Schematic representation of protein domains and N-glycosites. (d–f) Summary of LC-ESI-MS/MS analysis of N-glycan structures for adalimumab, SARS-CoV-2 receptor binding domain (RBD) and GOx glycosites. N-glycans are presented as a % of all structures reported at each N-glycosite. EndoH, endoglycosidase H; +/- glycosidase treatment; GOx, glycoprotein glucose oxidase; LC-ESI-MS/MS, liquid chromatography electrospray ionization tandem mass spectrometric; PNGase F, peptide:N-glycosidase F.

and with different HaloTag and Strep-II tag conformations. Antigen reactivity to two commercial antibodies was initially assessed, selected based on the recognition of either linear or conformational RBD epitopes. We observed similar reactivity of both antibodies against recombinantly expressed RBD and S1 from both BYL CFPS

and HEK293 cells (Figure 6c). Importantly, the reactivity against S1 was weaker than that for RBD.

Furthermore, to demonstrate true biological relevance of proteins produced in BYL, we found clear serological reactivity of the antigen samples (Figure 6d). An adapted ELISA workflow utilizing SARS-CoV-2

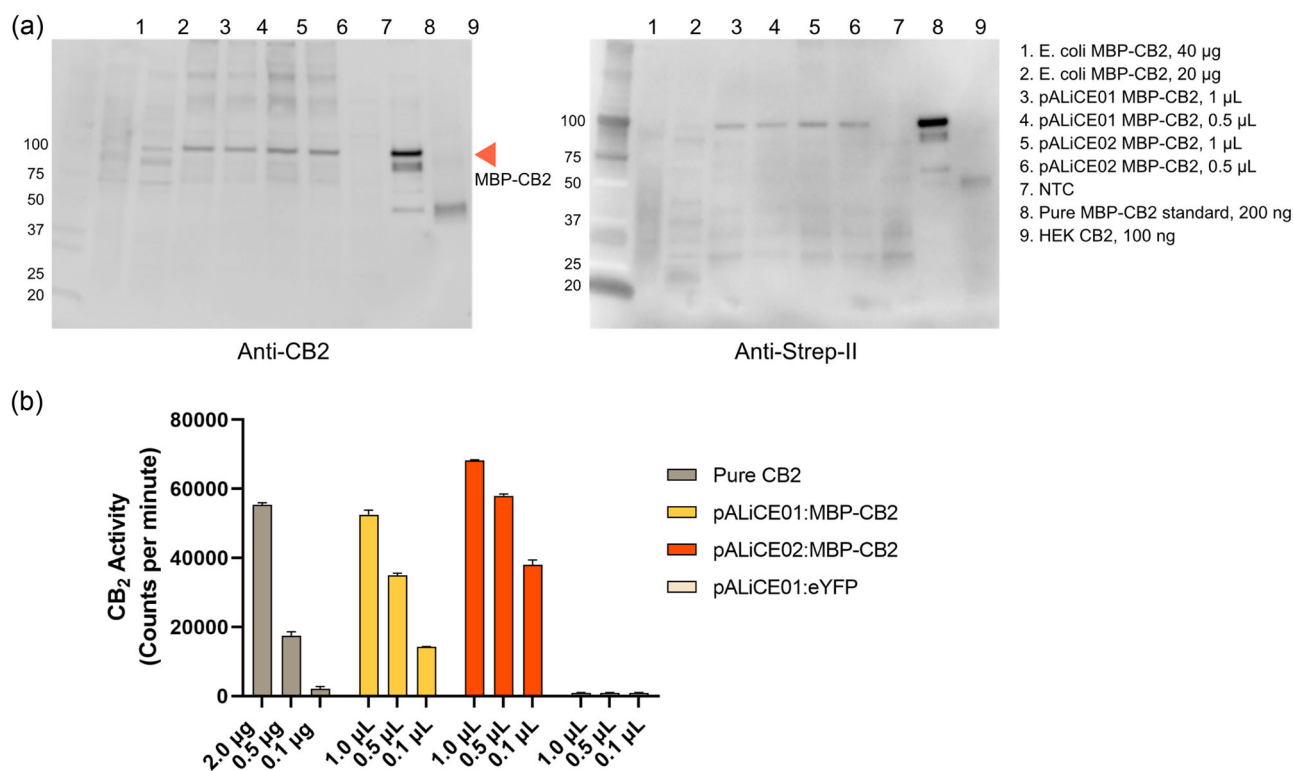


FIGURE 5 Expression and activity assays of human cannabinoid receptor CB2 expressed in BYL. (a) Western blot analysis with anti-CB2 and anti-Strep-II tag antibodies. Volumes of either 0.5 or 1.0 μL of crude BYL were applied with a DNA-free negative control and MBP-CB2 positive controls from *Escherichia coli* and HEK expression. The expected molecular weight of the MBP-CB2 fusion protein is indicated as 88 kDa. (b) CB2 activation assay from CP-55,940 scintillation counts. Bars represent average values and standard deviations from four independent measurements. CB2, cannabinoid receptor type 2; HEK, human embryonic kidney; MBP, maltose-binding protein.

patient serum antibodies showed that the RBD produced in BYL was directly comparable to that of RBD produced in HEK293 cells. Interestingly, higher reactivity was observed for COVID-19 patient samples but lower reactivity for samples collected from control subjects before 2019, and this separation was less significant for S1 antigens. Different C-terminal Strep-II tag and HaloTag configurations did not affect binding, suggesting correct RBD folding independent of fusion protein additions. This experiment suggests the use of RBD produced using BYL for therapeutic purposes and scaled expression for animal studies should be a priority for future research.

Finally, hEGF has been extensively investigated for its potential ability to promote rapid healing of serious injuries, such as cuts, burns, and diabetic ulcers (Yamakawa & Hayashida, 2019). Although hEGF promises potential clinical value, the growth factor is restricted to the treatment of chronic diabetic ulcers because of its high production cost and poor stability. Mature hEGF is a complex peptide of 53 amino acids that possess three intramolecular disulfide bonds. It was chosen as a model protein to challenge the capabilities of the BYL system as an alternative expression host for bioactive hEGF (Ogiso et al., 2002).

The hEGF gene with an N-terminal Strep-II tag was cloned into pALiCE02 for microsomal expression. Single-step streptavidin affinity purification was sufficient to extract soluble hEGF at high purity (Figure 6e). Binding of the purified protein to the cognate EGFR was used as a surrogate measure of bioactivity and analyzed by SPR

(Figure 6f). hEGF expressed in the BYL showed comparable or improved binding kinetics compared to a commercial hEGF reference product expressed from *E. coli*, suggesting correct folding and disulfide bond formation. Prokaryotic CFPS systems require extensive engineering to enable disulfide bond formation that can be circumvented by the use of BYL microsomes.

4 | DISCUSSION

The promise of cell-free systems is acceleration of the protein biotechnology industry—anything that can be done using cells could be done faster, with lower technical and infrastructural barriers to entry using CFPS. Cell-free production of protein therapeutics and drug screening targets are clear opportunities but the fields of synthetic biology, metabolic engineering, structural biology, and more all stand to benefit. However, despite many reports of independently produced cell-free lysates derived from multiple organisms, and the increasing commercial availability of cell-free kits, broad uptake of the technology in academic and industrial sectors has lagged. Major challenges still exist for CFPS in terms of batch-to-batch consistency, yield, scalability, cost effectiveness, protein folding, and protein functionality. Herein, we have disclosed the results of a decade-long development path toward solving these issues in the BY-2 cell lysate that is commercialized as

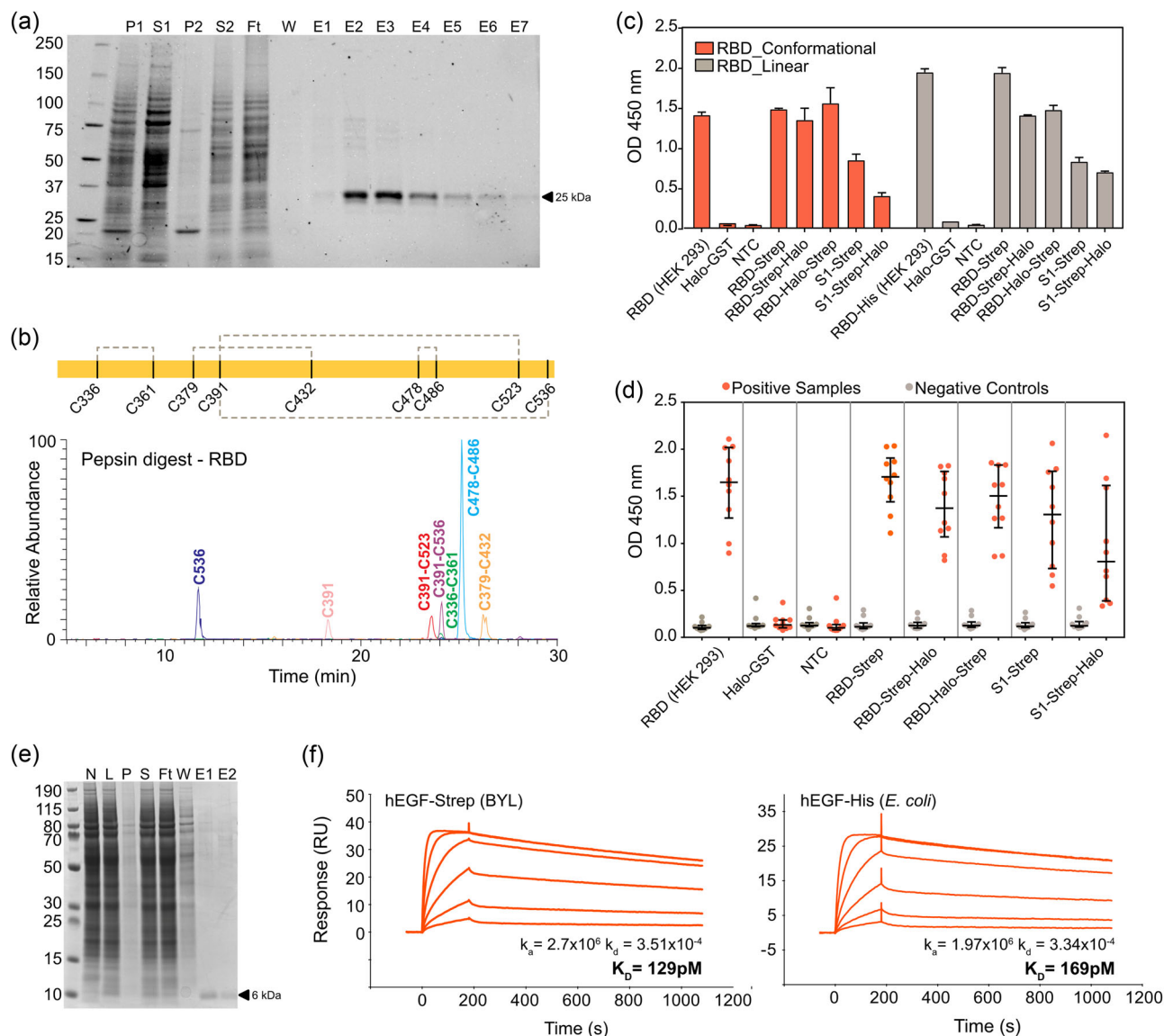


FIGURE 6 (a) SDS-PAGE of RBD purification fractions. (b) Disulfide bond analysis of RBD. (c) Binding assays of BYL-derived SARS-CoV-2 antigens with commercial anti-RBD antibodies specific for either the conformational epitope of correctly folded RBD (orange) or a linear epitope of RBD based on primary amino acid sequence (gray). An ELISA format was applied, with optical density readings at 450 nm wavelength (OD 450 nm) used as the quantitative readout, data represent average values and standard deviations from three independent measurements. (d) Serology-based ELISA of SARS-CoV-2 antigen binding. Serum samples were obtained from human patients who tested positive (orange) or negative (gray) for COVID-19 infection (readout at OD 450 nm). (e) SDS-PAGE of hEGF purification fractions. (f) SPR comparison of hEGF produced in either BYL or *Escherichia coli*. CFPS, cell-free protein synthesis; E1/E2, elution fractions; E1-E7, elution fractions; Ft, resin flow through; hEGF, human epidermal growth factor; L, BYL lysate after CFPS reaction; N, BYL non-template control; P, insoluble fraction pellet; P1/P2, insoluble fraction pellets; RBD, receptor-binding domain; S, soluble fraction; SPR, surface plasmon resonance; S1/S2, soluble fractions; W, wash.

ALiCE.[®] Using multiple batches of the publicly available, commercial-grade lysate, functional expression of an: enzyme, monoclonal antibody, viral antigen, VLP, and membrane protein was achieved, with inter-batch comparability demonstrated across protein quality metrics of glycosylation and disulfide bonding (protein targets summarized in Supporting Information: Table 2).

Linear, lossless scaling of reactions for reporter proteins across microliter to milliliter volumes has also been shown, to include 1 L

reactions from a recently scaled lysate production methodology. Reactions were performed in batch mode by simply combining lysate with template DNA and incubating the mixtures, albeit with specific bioreactor equipment requirements at the liter scale. Despite the large 20,000x scaling factor, rigorous process development was not needed and translating conditions suggested from the literature was sufficient for the Erlenmeyer and CELL-tainer[®] CT20 vessels. However, it is worth noting the system-specific requirement for

oxygenation. BYL does not provide optimal yields in an anaerobic reaction mode, as mitochondria are required to generate the intermediary energy substrates that power the transcription-translation reaction over the 48 h timeframe. This is actually beneficial for the scaling potential of the system, as preserved mitochondrial function lowers upfront reaction mix demands for cost-prohibitive chemical energy supplementation.

Other conceptual challenges emerge when considering the widespread adoption of liter scale CFPS reactions for example, template DNA supply. Milligram quantities of pure plasmid are required to drive these reactions which pushes lab-scale plasmid purification to its limits. GMP grade material may also be necessary where biomanufacturing of human therapeutics are concerned. Fortunately, the fields of gene therapy and mRNA vaccine manufacturing have rapidly grown in recent years, with an auxiliary DNA manufacturing sector emerging as an added benefit. Recent process economics modeling approaches have also favorably evaluated the switch to CFPS from traditional cell-based biomanufacturing, especially in terms of lessened personnel and facility costs for protein expression reactions that are completed in days, instead of upstream workflows that require weeks (Stamatis & Farid, 2021). Additional incorporation of operational benefits such as safety and product-agnostic flexibility for the manufacture of multiple highly toxic neurotoxin products resulted in unequivocal support for CFPS over a cell-based system (Olughu et al., 2022). However, it is difficult to truly obtain a cost per unit of protein as biomanufacturing with CFPS is a newly emerging field. It is expected that the first clinical approval for a CFPS-derived therapeutic or vaccine will come from ongoing clinical trials from Sutro Biopharma or Vaxcyte, respectively, thus validating the technology as a viable alternative to the predominant cell-based paradigm. Both companies use the XpressCF™ platform but as this system is not openly available for purchase then no price is available for direct cost comparisons.

The varied proteins expressed in this study were produced within 48 h reaction timeframes from off-the-shelf lysate starting material. However, as an open system, CFPS possesses deep opportunities for protein-specific optimization for enhanced yields and quality attributes. Reactions can be abstracted as chemoenzymatic processes instead of biological “black boxes,” permitting more extensive physicochemical interventions without consideration of cell walls or membranes for example, modulation of physicochemical parameters of pH and temperature, or the facile addition of cofactor and chaperone molecules (Tinafar et al., 2019). Some biological complexity cannot be escaped in the BYL system, particularly as it derives from whole cells. Glycosylation-competent microsomes, for example, are a major benefit of using eukaryotic CFPS over prokaryotic or reconstituted systems, and so a deeper characterization of BYL microsomes is planned to support biomanufacturing applications for example, lipidomic profiling of microsomes or physical determination of vesicle size profiles.

Short expression reactions are not the only point where CFPS offers acceleration, as these system entirely replace the need for

upstream development considerations of transfection, selection, and expansion of clones. This circumvents confounding variables like transfection efficiencies, indicating a more flexible screening platform than cell-based methods and with particular relevance to the monoclonal antibody discovery sector, especially as our CB2 work shows that function can be assessed in-lysate without purification. Streamlined protein variant expression also has relevance to pandemic preparedness for example, rapid production of SARS-CoV-2 RBD mutants from emerging viral strains for diagnostic or therapeutic purposes (Ramm et al., 2022). The use of CFPS has even been posited for individualized vaccines and distributed medicines manufacturing, presenting new medical paradigms if regulation can be safely adapted to meet this potential (Kanter et al., 2007; Ogonah et al., 2017; Zawada et al., 2022). The ALiCE® system has specifically been considered for the distributed manufacturing of the antiviral protein griffithsin, with equivalent bioactivity to griffithsin produced in *E. coli* CFPS (Borhani et al., 2023). We have also demonstrated the production of approximately 100,000 potential doses of the HBc VLP from a 1 L BYL reaction (Armero-Gimenez et al., 2023). Further acceleration of BYL workflows are in development to expand upon this potential, such as the application of alternative DNA templates beyond the standard plasmid format. Taking inspiration from *E. coli* CFPS, there are a variety of strategies that could be trialed for adapting linear DNA templates in BYL (Fochtman & Oza, 2023; Sato et al., 2022; Zhu et al., 2020).

For this study, eukaryotic model proteins were deliberately chosen to challenge the capabilities of the system. We have shown that BYL can produce functional proteins as diverse as enzymes, multi-pass transmembrane GPCRs, small, soluble growth factors, and immunologically-active viral antigens. Moreover, functional expression of various biosynthetic enzymes, Cas9 nuclease and the antibody M12 have previously been reported from BYL (Buntru et al., 2015, 2022; Schiermeyer et al., 2022). Protein function is intrinsically linked to correct folding but further molecular characterization was warranted to prove that the microsomes of this eukaryotic CFPS system are able to produce recombinant proteins at the same quality as a cell and with batch-to-batch consistency. Essential features such as N-linked glycosylation are not possible in prokaryotic CFPS without extensive engineering but was confirmed herein with high structural homogeneity and N-glycosite occupancy. High-mannose structures typical of plant N-glycosylation were understandably prevalent, considering the BY-2 cell culture starting material. Humanized glycosylation strategies are being explored for applications where the functional relevance of N-glycosylation is more important for example, antibody-dependent cell-mediated cytotoxicity. There is a strong field of *Nicotiana* spp. and BY-2 cell glycoengineering from which to draw upon (Dicker et al., 2016; Kallolimath et al., 2016; Schoberer & Strasser, 2018; Strasser et al., 2008; Yin et al., 2011), and we have already produced BYL from cells with genetic knock-out of plant-specific xylosyl- and fucosyltransferases.

Regardless of expression host, membrane proteins are universally considered as particularly challenging targets for recombinant expression due to specific requirements for folding, PTMs, and correct insertion into cell membranes or detergent micelles (Bernaudo et al., 2011; Grishammer, 2006). Indeed, membrane proteins are underrepresented in the Protein Data Bank, despite constituting about 30% of the human proteome. This gap is of keen interest for the pharmaceutical industry, as 50% of approved pharmaceutical molecules target membrane proteins (Birch et al., 2020). Functional CB2 was expressed in this study using the standard format of BYL lysate, without supplementation of exogenous lipidic platforms or detergents, and performed equally or better than the same construct produced in standard *E. coli* culture. Additional work could be required to solubilize CB2 for the various screening and structural biology workflows that are utilized in small molecule drug discovery but it is encouraging that functional starting material can be easily obtained in BYL, whereby necessary overexpression of membrane proteins has been repeatedly posited as toxic to cell-based systems. With increasing reports of functional GPCR expression in cell-free systems, it is envisaged that this knowledge gap between membrane protein genomics and useful structures with soon be bridged by CFPS (Khambhati et al., 2019).

Beyond proteins as target molecules, cell-free is also proving useful for prototyping of biosynthetic enzyme pathways for the production of high-value chemicals (Buntru et al., 2022; Liew et al., 2022). Prototyping is enabled by throughput and whilst microfluidics show increasing potential for CFPS workflows, the equipment is broadly inaccessible in standardized laboratory setups. More universal multiwell-based screening platforms require large volumes of high-yielding lysate with dependably reproducible quality to effectively sample the immense experimental design space when reengineering multistep biosynthetic pathways. Within these contexts, our lossless scaling results also suggest BYL as an end-to-end R&D to manufacturing platform. First-line protein engineering and lead development activities are achievable on the microscale before transitioning to gram scale production of protein material, without requiring extensive process development and optimization. CFPS has the potential to accelerate R&D pipelines for faster time-to-market turnaround of novel protein therapeutics, diagnostics, and even high value small molecules.

ACKNOWLEDGMENTS

We thank our colleagues at LenioBio for their support and expertise during the performance of this research. We greatly appreciate the contribution of Dr. Jan W. M. van Lent and the Wageningen Electron Microscopy Center (WEMC), Wageningen, Netherlands for the electron microscopy pictures and wish him a very happy retirement. Thanks also to Clemens Grünwald-Gruber and the Mass Spectrometry core facility of BOKU, Austria for their work in mass spectrometry analyses. This project has received funding from the European Union's Horizon 2020 research and innovation program, under grant agreement No 881025 "PEPPER," and from the German BMBF Bioökonomie No 0312B083OB "ThinkBig" project.

CONFLICTS OF INTEREST STATEMENT

M. D. G., Y. F., R. R., H. J., J. A. G., F. A., J. H., Z. A. A., J. N., C. W., and R. F. were employed by LenioBio GmbH at the time of their contributions. R. F. is also a stakeholder in the company. The remaining authors declare no conflict of interest.

DATA AVAILABILITY STATEMENT

Research data are not shared.

ORCID

Charles Williams  <http://orcid.org/0000-0001-7781-8693>

REFERENCES

- Armero-Gimenez, J., Wilbers, R., Schots, A., Williams, C., & Finnern, R. (2023). Rapid screening and scaled manufacture of immunogenic virus-like particles in a tobacco BY-2 cell-free protein synthesis system. *Frontiers in Immunology*, 14, 296. <https://doi.org/10.3389/FIMMU.2023.108852/BIBTEX>
- Aw, R., Spice, A. J., & Polizzi, K. M. (2020). Methods for expression of recombinant proteins using a *Pichia pastoris* cell-free system. *Current Protocols in Protein Science*, 102(1), e115. <https://doi.org/10.1002/cpps.115>
- Beckner, R. L., Zoubak, L., Hines, K. G., Gawrisch, K., & Yeliseev, A. A. (2020). Probing thermostability of detergent-solubilized CB2 receptor by parallel G protein-activation and ligand-binding assays. *Journal of Biological Chemistry*, 295(1), 181–190. <https://doi.org/10.1074/JBC.RA119.010696>
- Bernaudo, F., Frelet-Barrand, A., Pochon, N., Dementin, S., Hivin, P., Boutigny, S., Rioux, J. B., Salvi, D., Seigneurin-Berny, D., Richaud, P., Joyard, J., Pignol, D., Sabaty, M., Desnos, T., Pebay-Peyroula, E., Darrouzet, E., Vernet, T., & Rolland, N. (2011). Heterologous expression of membrane proteins: Choosing the appropriate host. *PLoS ONE*, 6(12), e29191. <https://doi.org/10.1371/JOURNAL.PONE.0029191>
- Birch, J., Cheruvara, H., Gamage, N., Harrison, P. J., Lithgo, R., & Quigley, A. (2020). Changes in membrane protein structural biology. *Biology*, 9(11), 401. <https://doi.org/10.3390/BIOLOGY9110401>
- Borhani, S. G., Levine, M. Z., Krumpke, L. H., Wilson, J., Henrich, C. J., O'Keefe, B. R., Lo, D. C., Sittampalam, G. S., Godfrey, A. G., Lunsford, R. D., Mangalampalli, V., Tao, D., LeClair, C. A., Thole, A. P., Frey, D., Swartz, J., & Rao, G. (2023). An approach to rapid distributed manufacturing of broad spectrum anti-viral griffithsin using cell-free systems to mitigate pandemics. *New Biotechnology*, 76, 13–22. <https://doi.org/10.1016/J.NBT.2023.04.003>
- Brödel, A. K., Sonnabend, A., & Kubick, S. (2014). Cell-free protein expression based on extracts from CHO cells. *Biotechnology and Bioengineering*, 111(1), 25–36. <https://doi.org/10.1002/BIT.25013>
- Büchs, J., Maier, U., Milbradt, C., & Zoels, B. (2000). Power consumption in shaking flasks on rotary shaking machines: I. Power consumption measurement in un baffled flasks at low liquid viscosity. *Biotechnology and Bioengineering*, 68, 589–593. [https://doi.org/10.1002/\(SICI\)1097-0290\(20000620\)68:6](https://doi.org/10.1002/(SICI)1097-0290(20000620)68:6)
- Buntru, M., Hahnengress, N., Croon, A., & Schillberg, S. (2022). Plant-derived cell-free biofactories for the production of secondary metabolites. *Frontiers in Plant Science*, 12, 3282. <https://doi.org/10.3389/FPLS.2021.794999/BIBTEX>
- Buntru, M., Vogel, S., Finnern, R., & Schillberg, S. (2022). Plant-based cell-free transcription and translation of recombinant proteins. *Methods in Molecular Biology*, 2480, 113–124. https://doi.org/10.1007/978-1-0716-2241-4_8/FIGURES/3
- Buntru, M., Vogel, S., Spiegel, H., & Schillberg, S. (2014). Tobacco BY-2 cell-free lysate: An alternative and highly-productive plant-based in

- vitro translation system. *BMC Biotechnology*, 14, 37. <https://doi.org/10.1186/1472-6750-14-37>
- Buntru, M., Vogel, S., Stoff, K., Spiegel, H., & Schillberg, S. (2015). A versatile coupled cell-free transcription-translation system based on tobacco BY-2 cell lysates. *Biotechnology and Bioengineering*, 112(5), 867–878. <https://doi.org/10.1002/bit.25502>
- Carlson, E. D., Gan, R., Hodgman, C. E., & Jewett, M. C. (2012). Cell-free protein synthesis: Applications come of age. *Biotechnology Advances*, 30(5), 1185–1194. <https://doi.org/10.1016/j.biotechadv.2011.09.016>
- Caschera, F., & Noireaux, V. (2014). Synthesis of 2.3 mg/ml of protein with an all *Escherichia coli* cell-free transcription-translation system. *Biochimie*, 99(1), 162–168. <https://doi.org/10.1016/j.biochi.2013.11.025>
- Colant, N., Melinek, B., Teneb, J., Goldrick, S., Rosenberg, W., Frank, S., & Bracewell, D. G. (2021). A rational approach to improving titer in *Escherichia coli*-based cell-free protein synthesis reactions. *Biotechnology Progress*, 37(1), e3062. <https://doi.org/10.1002/BTPR.3062>
- Dicker, M., Tschofen, M., Maresch, D., König, J., Juarez, P., Orzaez, D., Altmann, F., Steinkellner, H., & Strasser, R. (2016). Transient glyco-engineering to produce recombinant IgA1 with defined N- and O-glycans in plants. *Frontiers in Plant Science*, 7, 18. <https://doi.org/10.3389/fpls.2016.00018>
- Dickey, T. H., Tang, W. K., Butler, B., Ouahes, T., Orr-Gonzalez, S., Salinas, N. D., Lambert, L. E., & Tolia, N. H. (2022). Design of the SARS-CoV-2 RBD vaccine antigen improves neutralizing antibody response. *Science Advances*, 8(37), eabq8276. https://doi.org/10.1126/SCIADV.ABQ8276/SUPPL_FILE/SCIADV.ABQ8276_SM.PDF
- Dondapati, S. K., Stech, M., Zemella, A., & Kubick, S. (2020). Cell-free protein synthesis: A promising option for future drug development. *BioDrugs*, 34(3), 327–348. <https://doi.org/10.1007/s40259-020-00417-y>
- Ezure, T., Suzuki, T., Higashide, S., Shintani, E., Endo, K., Kobayashi, S., Shikata, M., Ito, M., Tanimizu, K., & Nishimura, O. (2006). Cell-free protein synthesis system prepared from insect cells by freeze-thawing. *Biotechnology Progress*, 22(6), 1570–1577. <https://doi.org/10.1021/BP060110V>
- Fochtman, T. J., & Oza, J. P. (2023). Established and emerging methods for protecting linear DNA in cell-free expression systems. *Methods and Protocols*, 6(2), 36. <https://doi.org/10.3390/MP56020036>
- Gregorio, N. E., Levine, M. Z., & Oza, J. P. (2019). A user's guide to cell-free protein synthesis. *Methods and Protocols*, 2(1), 24. <https://doi.org/10.3390/mps2010024>
- Grisshammer, R. (2006). Understanding recombinant expression of membrane proteins. *Current Opinion in Biotechnology*, 17(4), 337–340. <https://doi.org/10.1016/j.copbio.2006.06.001>
- Harbers, M. (2014). Wheat germ systems for cell-free protein expression. *FEBS Letters*, 588(17), 2762–2773. <https://doi.org/10.1016/j.febslet.2014.05.061>
- He, Y., Qi, J., Xiao, L., Shen, L., Yu, W., & Hu, T. (2021). Purification and characterization of the receptor-binding domain of SARS-CoV-2 spike protein from *Escherichia coli*. *Engineering in Life Sciences*, 21(6), 453–460. <https://doi.org/10.1002/ELSC.202000106>
- Kallolmuth, S., Castilho, A., Strasser, R., Grünwald-Gruber, C., Altmann, F., Strubl, S., Galuska, C. E., Zlatina, K., Galuska, S. P., Werner, S., Thiesler, H., Werneburg, S., Hildebrandt, H., Gerardy-Schahn, R., & Steinkellner, H. (2016). Engineering of complex protein sialylation in plants. *Proceedings of the National Academy of Sciences*, 113(34), 9498–9503. <https://doi.org/10.1073/pnas.1604371113>
- Kanter, G., Yang, J., Voloshin, A., Levy, S., Swartz, J. R., & Levy, R. (2007). Cell-free production of scFv fusion proteins: An efficient approach for personalized lymphoma vaccines. *Blood*, 109(8), 3393–3399. <https://doi.org/10.1182/blood-2006-07-030593>
- Khambhati, K., Bhattacharjee, G., Gohil, N., Braddick, D., Kulkarni, V., & Singh, V. (2019). Exploring the potential of cell-free protein synthesis for extending the abilities of biological systems. *Frontiers in Bioengineering and Biotechnology*, 7, 248. <https://doi.org/10.3389/fbioe.2019.00248>
- Kirchhoff, J., Raven, N., Boes, A., Roberts, J. L., Russell, S., Treffenfeldt, W., Fischer, R., Schinkel, H., Schiermeyer, A., & Schillberg, S. (2012). Monoclonal tobacco cell lines with enhanced recombinant protein yields can be generated from heterogeneous cell suspension cultures by flow sorting. *Plant Biotechnology Journal*, 10(8), 936–944. <https://doi.org/10.1111/J.1467-7652.2012.00722.X>
- Kirchhoff, J., Schiermeyer, A., Schneider, K., Fischer, R., Ainley, W. M., Webb, S. R., Schinkel, H., & Schillberg, S. (2020). Gene expression variability between randomly and targeted transgene integration events in tobacco suspension cell lines. *Plant Biotechnology Reports*, 14(4), 451–458. <https://doi.org/10.1007/S11816-020-00624-7/FIGURES/3>
- Knauer, J. F., Liers, C., Hahn, S., Wuestenhagen, D. A., Zemella, A., Kellner, H., Haueis, L., Hofrichter, M., & Kubick, S. (2022). Cell-free production of the bifunctional glycoside hydrolase GH78 from *Xylaria polymorpha*. *Enzyme and Microbial Technology*, 161, 110110. <https://doi.org/10.1016/J.ENZMICTEC.2022.110110>
- Liew, F. E., Nogle, R., Abdalla, T., Rasor, B. J., Canter, C., Jensen, R. O., Wang, L., Strutz, J., Chirania, P., De Tissera, S., Mueller, A. P., Ruan, Z., Gao, A., Tran, L., Engle, N. L., Bromley, J. C., Daniell, J., Conrado, R., Tschaplinski, T. J., ... Köpke, M. (2022). Carbon-negative production of acetone and isopropanol by gas fermentation at industrial pilot scale. *Nature Biotechnology*, 40(3), 335–344. <https://doi.org/10.1038/s41587-021-01195-w>
- Lingappa, J. R., Martin, R. L., Wong, M. L., Ganem, D., Welch, W. J., & Lingappa, V. R. (1994). A eukaryotic cytosolic chaperonin is associated with a high molecular weight intermediate in the assembly of hepatitis B virus capsid, a multimeric particle. *Journal of Cell Biology*, 125(1), 99–111. <https://doi.org/10.1083/JCB.125.1.99>
- Maier, U., & Büchs, J. (2001). Characterisation of the gas-liquid mass transfer in shaking bioreactors. *Biochemical Engineering Journal*, 7(2), 99–106. [https://doi.org/10.1016/S1369-703X\(00\)00107-8](https://doi.org/10.1016/S1369-703X(00)00107-8)
- Mikami, S., Masutani, M., Sonenberg, N., Yokoyama, S., & Imataka, H. (2006). An efficient mammalian cell-free translation system supplemented with translation factors. *Protein Expression and Purification*, 46(2), 348–357. <https://doi.org/10.1016/J.PEP.2005.09.021>
- Min, L., & Sun, Q. (2021). Antibodies and vaccines target RBD of SARS-CoV-2. *Frontiers in Molecular Biosciences*, 8, 247. <https://doi.org/10.3389/FMOLB.2021.671633/BIBTEX>
- Nooraei, S., Bahrulolum, H., Hoseini, Z. S., Katalani, C., Hajizade, A., Easton, A. J., & Ahmadian, G. (2021). Virus-like particles: Preparation, immunogenicity and their roles as nanovaccines and drug nanocarriers. *Journal of Nanobiotechnology*, 19(1), 59. <https://doi.org/10.1186/S12951-021-00806-7>
- Ogiso, H., Ishitani, R., Nureki, O., Fukai, S., Yamanaka, M., Kim, J.-H., Saito, K., Sakamoto, A., Inoue, M., Shirouzu, M., & Yokoyama, S. (2002). Crystal structure of the complex of human epidermal growth factor and receptor extracellular domains. *Cell*, 110(6), 775–787. [https://doi.org/10.1016/S0092-8674\(02\)00963-7](https://doi.org/10.1016/S0092-8674(02)00963-7)
- Ogonah, O. W., Polizzi, K. M., & Bracewell, D. G. (2017). Cell free protein synthesis: A viable option for stratified medicines manufacturing. *Current Opinion in Chemical Engineering*, 18, 77–83. <https://doi.org/10.1016/j.coche.2017.10.003>
- Olughu, W., Stamatis, C., Farid, S., & Gruber, D. (2022). Cell-free synthesis of recombinant neurotoxins. *BioProcess International*, 20(11–12). <https://bioprocessintl.com/manufacturing/emerging-therapeutics-manufacturing/cell-free-synthesis-of-highly-potent-recombinant-neurotoxins-a-process-economic-feasibility-study/>
- Oosterhuis, N., & Junne, S. (2013–2014). *E. coli* cultivation in a 12L and 120L CELL-tainer™ single-use bioreactor. *BioProcess International*, 27.
- Orbán, E., Proverbio, D., Haberstock, S., Dötsch, V., & Bernhard, F. (2015). Cell-free expression of G-protein-coupled receptors. *Methods in Molecular Biology*, 1261, 171–195. https://doi.org/10.1007/978-1-4939-2230-7_10

- Piccoli, L., Park, Y. J., Tortorici, M. A., Czudnochowski, N., Walls, A. C., Beltramello, M., Silacci-Fregni, C., Pinto, D., Rosen, L. E., Bowen, J. E., Acton, O. J., Jaconi, S., Guarino, B., Minola, A., Zatta, F., Sprugasci, N., Bassi, J., Peter, A., De Marco, A., ... Veesler, D. (2020). Mapping neutralizing and immunodominant sites on the SARS-CoV-2 spike receptor-binding domain by structure-guided high-resolution serology. *Cell*, 183(4), 1024–1042. <https://doi.org/10.1016/J.CELL.2020.09.037>
- Ramm, F., Dondapati, S. K., Trinh, H. A., Wenzel, D., Walter, R. M., Zemella, A., & Kubick, S. (2022). The potential of eukaryotic cell-free systems as a rapid response to novel zoonotic pathogens: Analysis of SARS-CoV-2 viral proteins. *Frontiers in Bioengineering and Biotechnology*, 10, 617. <https://doi.org/10.3389/FBIOE.2022.896751/BIBTEX>
- Sato, W., Sharon, J., Deich, C., Gaut, N., Cash, B., Engelhart, A. E., & Adamala, K. P. (2022). Akaby—Cell-free protein expression system for linear templates. *PLoS ONE*, 17(4), e0266272. <https://doi.org/10.1371/JOURNAL.PONE.0266272>
- Schiermeyer, A., Cerda-Bennasser, P., Schmelter, T., Huang, X., Christou, P., & Schillberg, S. (2022). Rapid production of SaCas9 in plant-based cell-free lysate for activity testing. *Biotechnology Journal*, 17(7), 2100564. <https://doi.org/10.1002/BIOT.202100564>
- Schoberer, J., & Strasser, R. (2018). Plant glyco-biotechnology. *Seminars in Cell & Developmental Biology*, 80, 133–141. <https://doi.org/10.1016/j.semcdb.2017.07.005>
- Schwarz, D., Dötsch, V., & Bernhard, F. (2008). Production of membrane proteins using cell-free expression systems. *Proteomics*, 8(19), 3933–3946. <https://doi.org/10.1002/pmic.200800171>
- Spice, A. J., Aw, R., Bracewell, D. G., & Polizzi, K. M. (2020). Synthesis and assembly of hepatitis B virus-like particles in a *Pichia pastoris* cell-free system. *Frontiers in Bioengineering and Biotechnology*, 8, 72. <https://doi.org/10.3389/fbioe.2020.00072>
- Stamatis, C., & Farid, S. S. (2021). Process economics evaluation of cell-free synthesis for the commercial manufacture of antibody drug conjugates. *Biotechnology Journal*, 16(4), 2000238. <https://doi.org/10.1002/BIOT.202000238>
- Stech, M., Quast, R. B., Sachse, R., Schulze, C., Wüstenhagen, D. A., & Kubick, S. (2014). A continuous-exchange cell-free protein synthesis system based on extracts from cultured insect cells. *PLoS ONE*, 9(5), e96635. <https://doi.org/10.1371/journal.pone.0096635>
- Strasser, R., Stadlmann, J., Schäh, M., Stiegler, G., Quendler, H., Mach, L., Glössl, J., Weterings, K., Pabst, M., & Steinkellner, H. (2008). Generation of glyco-engineered *Nicotiana benthamiana* for the production of monoclonal antibodies with a homogeneous human-like N-glycan structure. *Plant Biotechnology Journal*, 6(4), 392–402. <https://doi.org/10.1111/j.1467-7652.2008.00330.x>
- Swartz, J. R. (2012). Transforming biochemical engineering with cell-free biology. *AIChE Journal*, 58(1), 5–13. <https://doi.org/10.1002/aic.13701>
- Tan, R. K., Eberhard, W., & Büchs, J. (2011). Measurement and characterization of mixing time in shake flasks. *Chemical Engineering Science*, 66(3), 440–447. <https://doi.org/10.1016/J.CES.2010.11.001>
- Tariq, H., Batool, S., Asif, S., Ali, M., & Abbasi, B. H. (2022). Virus-like particles: Revolutionary platforms for developing vaccines against emerging infectious diseases. *Frontiers in Microbiology*, 12, 4137. <https://doi.org/10.3389/FMICB.2021.790121/BIBTEX>
- Thoring, L., Dondapati, S. K., Stech, M., Wüstenhagen, D. A., & Kubick, S. (2017). High-yield production of 'difficult-to-express' proteins in a continuous exchange cell-free system based on CHO cell lysates. *Scientific Reports*, 7(1), 11710. <https://doi.org/10.1038/s41598-017-12188-8>
- Thoring, L., & Kubick, S. (2018). Versatile cell-free protein synthesis systems based on Chinese hamster ovary cells. *Methods in Molecular Biology*, 1850, 289–308. https://doi.org/10.1007/978-1-4939-8730-6_19
- Tinafar, A., Jaenes, K., & Pardee, K. (2019). Synthetic biology goes cell-free. *BMC Biology*, 17(1), 64. <https://doi.org/10.1186/s12915-019-0685-x>
- Xun, Y., Tremouilhac, P., Carraher, C., Gelhaus, C., Ozawa, K., Otting, G., Dixon, N. E., Leippe, M., Grötzinger, J., Dingley, A. J., & Kralicek, A. V. (2009). Cell-free synthesis and combinatorial selective ¹⁵N-labeling of the cytotoxic protein amoebapore A from *Entamoeba histolytica*. *Protein Expression and Purification*, 68(1), 22–27. <https://doi.org/10.1016/J.PEP.2009.06.017>
- Xu, Z., Chen, H., Yin, X., Xu, N., & Cen, P. (2005). High-level expression of soluble human beta-defensin-2 fused with green fluorescent protein in *Escherichia coli* cell-free system. *Applied Biochemistry and Biotechnology*, 127(1), 53–62. <https://doi.org/10.1385/ABAB:127:1:053>
- Yamakawa, S., & Hayashida, K. (2019). Advances in surgical applications of growth factors for wound healing. *Burns & Trauma*, 7, 10. <https://doi.org/10.1186/s41038-019-0148-1>
- Yeliseev, A. (2019). Expression and preparation of a G protein-coupled cannabinoid receptor CB2 for NMR structural studies. *Current Protocols in Protein Science*, 96(1), e83. <https://doi.org/10.1002/CPPS.83>
- Yeliseev, A., van den Berg, A., Zoubak, L., Hines, K., Stepnowski, S., Williston, K., Yan, W., Gawrisch, K., & Zmuda, J. (2020). Thermostability of a recombinant G protein-coupled receptor expressed at high level in mammalian cell culture. *Scientific Reports*, 10(1), 16805. <https://doi.org/10.1038/s41598-020-73813-7>
- Yeliseev, A., Zoubak, L., & Schmidt, T. G. M. (2017). Application of Strep-Tactin XT for affinity purification of Twin-Strep-tagged CB2, a G protein-coupled cannabinoid receptor. *Protein Expression and Purification*, 131, 109–118. <https://doi.org/10.1016/j.pep.2016.11.006>
- Yin, B. J., Gao, T., Zheng, N. Y., Li, Y., Tang, S. Y., Liang, L. M., & Xie, Q. (2011). Generation of glyco-engineered BY2 cell lines with decreased expression of plant-specific glycoepitopes. *Protein & Cell*, 2(1), 41–47. <https://doi.org/10.1007/S13238-011-1007-4>
- Zawada, J. F., Burgenson, D., Yin, G., Hallam, T. J., Swartz, J. R., & Kiss, R. D. (2022). Cell-free technologies for biopharmaceutical research and production. *Current Opinion in Biotechnology*, 76, 102719. <https://doi.org/10.1016/J.COPBIO.2022.102719>
- Zawada, J. F., Yin, G., Steiner, A. R., Yang, J., Naresh, A., Roy, S. M., Gold, D. S., Heinsohn, H. G., & Murray, C. J. (2011). Microscale to manufacturing scale-up of cell-free cytokine production—A new approach for shortening protein production development timelines. *Biotechnology and Bioengineering*, 108(7), 1570–1578. <https://doi.org/10.1002/bit.23103>
- Zhu, B., Gan, R., Cabezas, M. D., Kojima, T., Nicol, R., Jewett, M. C., & Nakano, H. (2020). Increasing cell-free gene expression yields from linear templates in *Escherichia coli* and *Vibrio natriegens* extracts by using DNA-binding proteins. *Biotechnology and Bioengineering*, 117(12), 3849–3857. <https://doi.org/10.1002/BIT.27538>

SUPPORTING INFORMATION

Additional supporting information can be found online in the Supporting Information section at the end of this article.

How to cite this article: Gupta, M. D., Flaskamp, Y., Roentgen, R., Juergens, H., Armero-Gimenez, J., Albrecht, F., Hemmerich, J., Arfi, Z. A., Neuser, J., Spiegel, H., Schillberg, S., Yeliseev, A., Song, L., Qiu, J., Williams, C., & Finner, R. (2023). Scaling eukaryotic cell-free protein synthesis achieved with the versatile and high-yielding tobacco BY-2 cell lysate. *Biotechnology and Bioengineering*, 1–17. <https://doi.org/10.1002/bit.28461>